Available online at www.sciencedirect.com
ScienceDirect
Geochimica et Cosmochimica Acta 72 (2008) 1660–1677
Geochimica et Cosmochimica Acta
www.elsevier.com/locate/gca

The Fe/Mn ratio in MORB and OIB determined by ICP-MS

Liping Qin [a,1], Munir Humayun [b,*]

[a] Department of the Geophysical Sciences, University of Chicago, Chicago, IL 60637, USA
[b] Department of Geological Sciences & National High Magnetic Field Laboratory, Florida State University, Tallahassee, FL 32310, USA

Received 13 November 2006; accepted in revised form 15 January 2008; available online 26 January 2008

Abstract

Variations in the abundance of iron in the mantle may have important consequences for mantle dynamics and geochemistry. The abundance of iron in lavas derived from mantle source regions varies during partial melting and subsequent fractionation, so that source heterogeneities are not easily resolved in iron abundances alone. However, manganese is a geochemically similar element, so that the planetary Fe/Mn ratio is approximately constant. Here, we report new Fe/Mn results for mid-oceanic ridge basalts (MORBs), oceanic island basalts (OIBs) and komatiites using a precise inductively coupled plasma mass spectrometric (ICP-MS) method to measure Fe/Mn to better than 0.5% (2σ). As a measure of reproducibility of Fe/Mn, five olivine and five orthopyroxene grains from a Kilbourne Hole peridotite xenolith yielded Fe/Mn 69.8 ± 0.4 and 44.3 ± 0.2, respectively. To avoid ubiquitous secondary Fe–Mn oxides, Fe/Mn ratios in Pacific, Atlantic, and Indian MORBs were determined by Laser Ablation ICP-MS. MORB Fe/Mn (53–56) corrected for crystal fractionation yielded a value of 54.0 ± 1.2 (1σ). Icelandic basalts and picrites (MgO 10–29%) had Fe/Mn ratios 56–61, with a single exception. Six relatively fresh komatiites from Belingwe (MgO 20–29%) yielded Fe/Mn values of 58.3 ± 0.2 (1σ). Basalts from Tahiti and Reunion exhibited high Fe/Mn (>65), like Hawaii. This implies that the mantle source regions of Tahiti and Reunion lavas may have been enriched in Fe relative to other mantle reservoirs (e.g., MORBs, Iceland, Belingwe). Combined with previous results for Hawaii, we now find that Fe/Mn > 65 is characteristic of at least two plumes from the Pacific Superswell. It is conceivable that this is evidence for excess Fe due to core–mantle interaction in these mantle plumes, although partial melting of secondary pyroxenites may cause similar variations in Fe/Mn. Heterogeneity of Fe/Mn in mantle-derived lavas is now clearly documented.

1. INTRODUCTION

It has long been speculated that the Earth's upper mantle is compositionally distinct from the lower mantle (Anderson, 1989). The upper mantle is sampled along active plate boundaries by mid-ocean ridge basalts (MORB), which reveal their source to be depleted in incompatible trace elements by prior melting of primitive upper mantle. Intraplate magmatism may sample compositional anomalies in the upper mantle, or entrained lower mantle material, the products of which are termed Ocean Island basalts (OIB). Compositionally, OIB magmas originate from mantle source regions enriched in incompatible trace elements that may be derived by recycling of subducted oceanic crust (Hofmann, 1997). Some OIBs, e.g., Hawaii, are thought to be generated by partial melting of mantle plumes originating in the deep mantle (Shen et al., 2003), probably from the core–mantle boundary (CMB), the major compositional and thermal boundary layer of the mantle (Jellinek and Manga, 2004). Seismic studies show that some mantle plumes, such as Hawaii and Iceland, may be rooted at the

* Corresponding author. Fax: +1 850 644 0827.
E-mail address: humayun@magnet.fsu.edu (M. Humayun).
[1] Present address. Department of Terrestrial Magnetism, Carnegie Institution of Washington, 5241 Broad Branch Road, NW, Washington, DC 20015, USA.

0016-7037/$ - see front matter © 2008 Elsevier Ltd. All rights reserved.
doi:10.1016/j.gca.2008.01.012

core–mantle boundary (Russell et al., 1998; Bijwaard and Spakman, 1999), although other studies indicate that the plume under Hawaii, but not that under Iceland originate at the CMB (Montelli et al., 2004).

Osmium isotopes show coupled enrichments in $^{186}Os/^{188}Os$ and $^{187}Os/^{188}Os$ in intraplate lavas from Noril'sk (Walker et al., 1997), Hawaii (Brandon et al., 1998, 1999), and Gorgona Island (Brandon et al., 2003), interpreted as a signature of core–mantle interaction. ^{186}Os is the decay product of ^{190}Pt and ^{187}Os is the decay product of ^{187}Re, so that the coupled variations imply Pt/Re ratios >80 for their sources that are much higher than those of typical crustal rocks (Pt/Re <30). Such high Pt/Re ratios are characteristic of differentiated iron meteorites, potential analogues of the Earth's differentiated outer core (Walker et al., 1997), and imply an addition of less than 1% outer core Os to the plume mantle (Brandon et al., 1999). This explanation requires the core to be an important player in mantle geochemistry (e.g., Walker, 2000; Brandon and Walker, 2005). This process may add iron to the mantle to the extent of less than 1%, which would perturb the primitive mantle's Fe abundance (6.26%; McDonough and Sun, 1995) by <16% relative.

Ravizza et al. (2001) observed Pt/Re >80 in Mn-sediments with radiogenic Os, and proposed that assimilation of ancient Mn-rich oceanic metalliferrous sediments by either basaltic melts or their source regions can potentially give rise to the Os isotope signature in Hawaiian picrites. Brandon et al. (2003) pointed out that elevated MnO abundances should be a consequence of adding significant quantities of Mn-rich sediments to a mantle plume, which was not observed in Gorgona komatiites.

A better tool for exploring additions of either Mn or Fe to typical mantle peridotites or basalts is the Fe/Mn ratio. Most of the Fe in the mantle is Fe^{2+} (e.g., Canil et al., 1994) and all Mn is Mn^{2+}; Fe^{2+} (0.078 nm) and Mn^{2+} (0.083 nm) have similar ionic radii (Henderson, 1982). The two elements also have similar distribution coefficients between solids and liquids (Humayun et al., 2004). Laul et al. (1972) demonstrated that Fe/Mn ratios in mantle-derived rocks within individual planetary bodies (Earth, Moon, eucrites) remain nearly constant. McDonough and Sun (1995) obtained an average upper mantle $Fe/Mn = 60 \pm 10$ (1σ) from a compilation of over 1300 peridotites, while Ruzicka et al. (2001) obtained an essentially identical $Fe/Mn = 59 \pm 9$ (1σ) from a compilation of terrestrial basalts. Further, Ruzicka et al. (2001) noted that Fe/Mn did not correlate with petrological indicators of degree of partial melting or fractional crystallization, but that there was an inverse correlation between Fe/Mn and MnO. They interpreted this correlation as an analytical artifact due to imprecise MnO abundance data for basalts.

Humayun et al. (2004) reported Fe/Mn ratios determined by magnetic-sector ICP-MS on Hawaiian lavas that showed variations in mantle source Fe/Mn ratios that would be obscured by the noise in previous datasets, confirming the observations of Ruzicka et al. (2001) that analytical artifacts were significant contributors to the Fe/Mn range obtained from published datasets. Further, the new data showed that Hawaiian lavas are higher in Fe/Mn (~67) than MORBs (~58) and Icelandic lavas (58–61), the latter with a similar MgO range to Hawaiian lavas. The evidence of high Fe/Mn ratios in Hawaiian lavas was interpreted as possible evidence of core–mantle interaction (Humayun et al., 2004). Sobolev et al. (2005, 2007) have proposed an alternative interpretation involving a two-stage melting of eclogite (pyroxenite) that is expected to yield melts with high Fe/Mn ratio. Huang et al. (2007) have shown that the high Fe/Mn is a feature shared by the Ko'olau lavas.

It is now important to know the global distribution of high Fe/Mn in mantle-derived melts. In this paper, we present new Fe/Mn analyses on a collection of samples from various locations, including ocean island basalts and picrites, komatiites, and separated minerals from a single Kilbourne Hole peridotite xenolith. We present new data on MORB glasses from the Pacific, Atlantic, and Indian Oceans by both solution nebulization and laser ablation ICP-MS to assess the effect of Mn-crusts on the measured Fe/Mn in MORBs. These results refine the MORB data used in Humayun et al. (2004). Ocean island basalts and picrites from Iceland, Tahiti, and St. Helena provide new constraints on the Fe/Mn ratios of plume-derived mantle melts. St. Helena is the HIMU end-member of ocean islands, and its lavas are characterized by very radiogenic Pb isotope signatures, thought to be the result of oceanic crust recycling (e.g., Zindler and Hart, 1986). Tahiti, like Hawaii, belongs to the Pacific Superswell (Jellinek and Manga, 2004). Komatiites from Alexo, Belingwe, and Gorgona were studied here to determine the effect of fractionation on Fe/Mn. A caveat, of course, is that komatiites are weathered and metamorphosed and the effects of such processes on Fe/Mn ratios are not known in detail.

2. SAMPLES AND ANALYTICAL METHODOLOGY

2.1. Samples

Pacific, Atlantic, and Indian MORB glass samples are dredged samples obtained from the National Museum of Natural History (NMNH), Smithsonian Institution (details in Appendix 1A). Major-element compositions for the Pacific MORB glasses were determined by electron microprobe at the University of Chicago. Major-element data for other MORBs were obtained from the Smithsonian's MORB database (Melson et al., 2002).

Icelandic picrites were collected by A. D. Brandon and previously analyzed for Os isotopes (Brandon et al., 2007) and platinum group element (PGE) abundances (Humayun et al., 2002). The samples represent Holocene lavas from the Reykjanes rift (Western Rift Zone, WRZ); Theistareykir (Northern Rift Zone, NRZ), and Skridufell due west of Hekla in Southern Iceland (Eastern Rift Zone, ERZ). Further details are given in Appendix 1B and Brandon et al. (2007).

St. Helena, Tahiti, and Reunion samples were obtained from the NMNH. Daly (1927) collected the St. Helena samples from three flows at or near the top of Ladder Hill. The Tahiti samples are from the J. P. Iddings collection at NMNH. Further details are given in Appendix 1C. Most

of the Tahiti samples were olivine-phyric basalts. Reunion Island (France) is part of the Mascarene Islands, Indian Ocean, east of Madagascar, and is an active hotspot. The sample from Reunion Island (NMNH#113259) is an olivine-phyric basalt from the active volcano Piton de la Fournaise, (21°14′00″ S, 055°43′00″ E).

Komatiites from Belingwe, Zimbabwe, were from the Onias and Tony's flows and have been analyzed for Re–Os systematics (Walker and Nisbet, 2002). Samples of the Onias flow came from the SASKMAR 1 drill core (Nisbet et al., 1987). Olivine phenocrysts are variably altered to serpentine, talc and magnetite (Nisbet et al., 1987). ZV-10 is a well-preserved hand specimen from the lower B2 zone of Tony's flow (Nisbet et al., 1987). The Alexo samples analyzed here came from drill core ALE-49-98 and have been previously described and analyzed by Puchtel et al. (2004a). The single Gorgona komatiite analyzed was spinifex-textured komatiite from the west coast of Gorgona Island (Revillon et al., 2000; Brandon et al., 2003).

Kilbourne Hole is a volcanic maar located in New Mexico, known for its spinel peridotite xenoliths. The eruption age is approximately 80 kyr. Five olivine and five orthopyroxene single crystals were hand-picked from a disaggregated spinel peridotite xenolith, 97-MH-6 (collected by M. Humayun).

2.2. Sample dissolution

All the dissolution operations were conducted in a Class 100 clean lab at the University of Chicago. Most samples were powdered before acid dissolution. Rock samples from Smithsonian Institution were crushed with an agate mortar and pestle and only fresh interior chips were picked for analysis. About 100 mg of glass, rock powder, or fresh chips, were dissolved in 4 ml HF–HNO_3 in a sealed Savillex™ PFA vessel on a hotplate at ~170–180 °C. The solutions were evaporated to dryness at ~100–110 °C and taken up in 6 ml of 6 N HCl. The solutions were centrifuged and the residues redissolved in 6 ml of 6 N HCl. Occasionally, grains of chromite were observed as insoluble residues in high-MgO samples. Since $FeCl_3$ is volatile, samples were never dried down from HCl solutions. The sample solutions were stored in 125 ml LDPE bottles stabilized by 5% HCl to prevent the precipitation of Fe and Mn.

A subset of the samples (six Iceland picrites) was also dissolved by aqua regia digestion in a carius tube to achieve complete digestion of chromite. The carius tube procedures followed methods previously described from this lab (Puchtel and Humayun, 2001; Puchtel et al., 2004a; Puchtel and Humayun, 2005). The tubes were opened and the aqua regia solution was diluted and centrifuged. The siliceous residue was then dissolved on a hotplate using HF–HNO_3, followed by re-dissolution in 6 N HCl as described above. Residues could not always be quantitatively removed from the carius tubes, as material tended to adhere to the walls of the tube.

2.3. Solution nebulization ICP-MS

The stock solutions were diluted by a factor of 20–40 in 2% HCl to produce a final solution with ~3 ppm Fe. The solutions were introduced into the ICP-MS using an ESI™ Low-Flow 100 μl/min PFA nebulizer and an ESI™ PFA spray chamber. The MCN-6000, a desolvating nebulizer, was not used after tests showed significant losses of Fe relative to Mn. A single-collector Finnigan Element1™ high-resolution ICP-MS, equipped with guard electrode, operated in low-resolution mode ($R = 300$), was used for Fe/Mn ratio determination using methods described previously (Humayun et al., 2004). The peaks $^{54}Fe^+$, $^{55}Mn^+$, and $^{57}Fe^+$ were monitored by electrically scanning the acceleration voltage (EScan mode) at 50 milliseconds/peak over 10% of the mass window, with 800 sweeps of the mass spectrum. The detector was set in Analog mode and typical counting rates for ^{55}Mn and ^{57}Fe were of the order of 10^7 cps or higher. Polyatomic isobaric interferences (ClO^+, ArN^+, ArO^+, and $ArOH^+$) from matrix were monitored by measuring 2% HCl reference solution and the blank levels on ^{55}Mn and ^{57}Fe peaks were about 2–3% of the sample intensities. The interference on ^{54}Fe was high enough to limit the precision on $^{54}Fe/^{55}Mn$ ratio. So, only $^{57}Fe/^{55}Mn$ ratios were used to determine Fe/Mn in the samples. Mn is monoisotopic, while ^{57}Fe is 2.119% of natural Fe so that for a Fe/Mn of 60, ^{55}Mn and ^{57}Fe have similar intensities. After correction for background count rates, the $^{57}Fe/^{55}Mn$ ratios were converted to Fe/Mn ratios by using a calibration curve. The calibration curve was constructed from the measured intensity ratios of $^{57}Fe/^{55}Mn$ of a series of gravimetrically prepared standards with Fe/Mn ratios

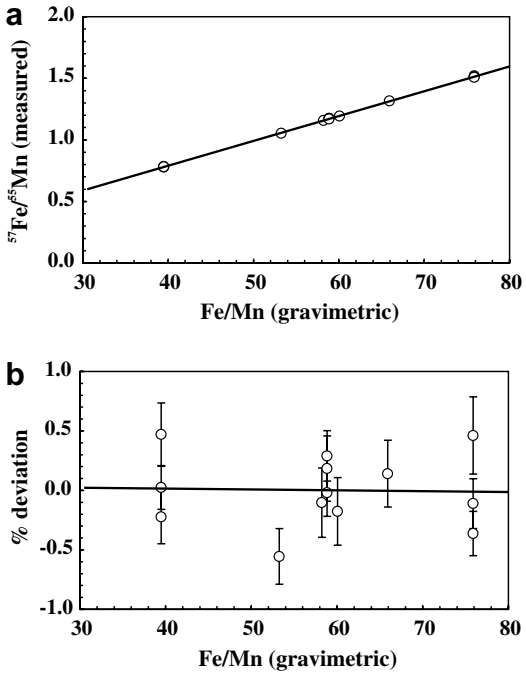

Fig. 1. Calibration curve for the Fe/Mn measurements: (a) comparison of the measured intensity ratio with the gravimetric value for seven standards. Three of the standards were measured in triplicate and are superposed over each other. (b) % deviation of the measured values from the calibration curve with internal run errors. The line is a linear regression to the data. Triplicates can now be seen as separate measurements.

from 40 to 80, constant Mn concentrations of ~0.05 ppm. The standards were prepared from Spex Certiprep™ high-purity solutions of Fe and Mn, and stabilized by 2% HCl to prevent precipitation of iron or manganese. In a typical analytical session, all the standards were first analyzed followed by a number of samples. The standards with Fe/Mn of 40, 60, and 80 were analyzed multiple times between samples to monitor instrumental drift. Fig. 1 shows a sample calibration curve used in this study. The reproducibility of the standards was generally within 0.5% (2σ), which also included uncorrected drift (Fig. 1).

2.4. Major-element analysis by ICP-MS

A number of samples, for which no major-element data were available, were analyzed for MgO, FeO_T and MnO by solution nebulization using the external standard method, where standards were prepared from Spex™ single-element solutions. The precision of the method was better than 5% (2σ). Where possible, MnO abundances were calculated from the Fe/Mn ratios and the FeO abundances and are shown as MnO_C.

2.5. Acid leaching procedure for MORBs

MORB samples have Fe–Mn hydroxides precipitated from seawater. These precipitates occur as Mn-crusts coating the outside of the MORB glasses, as veins along pervasive cracks through the glasses, and as vesicle linings. In the former case, the Fe–Mn crust can be physically removed. But pervasive veins or vesicle fillings required application of a leaching procedure adopted from Reinitz and Turekian (1989). About 100 mg of submillimeter-sized fresh chips were picked from interior portions of the glass samples, then treated with 0.1% HCl and 3% H_2O_2. The mixture was put into an ultrasonic bath for 30 min and then allowed to sit overnight. It was then centrifuged for 15 min, and the leachate decanted. The chips were leached a second time in the same manner using 0.1% HCl, to which a small amount of oxalic acid was added. This leachate was decanted to the container with the former leachate. The chips were then rinsed with 0.1% HCl several times and the rinse was added to the leachate. The residues were then dissolved in HF–HNO_3 following the procedure described above. The leachates and residues were analyzed by ICP-MS for Fe concentrations and Fe/Mn ratios.

2.6. Laser ablation ICP-MS analysis of MORBs

To determine whether the Fe/Mn ratios of MORBs were biased by the leaching procedure, the MORB glasses were also analyzed by laser ablation ICP-MS (LA-ICP-MS). A CETAC LSX-200, 266 nm UV laser ablation system, coupled to the Element1™, was used (Campbell and Humayun, 1999; Campbell et al., 2002). The beam diameter of the laser used in this study was 100μm, the energy level was 20 and the repetition rate was 10 Hz. Because the samples were relatively large (>1 mm), the line scan mode was used, in which the sample is moved under the laser by a motorized stage. The scanning speed was 20 μm/s. The Element1™ was operated in low-resolution ($R = 300$). The ^{57}Fe and ^{55}Mn peaks were acquired in EScan mode by 750 sweeps of the mass spectrum per line scan. For each analysis, five line scans were performed and the results averaged, analogous to precise LA-ICP-MS analyses performed on iron meteorites (Campbell and Humayun, 2005). The detector was set in Analog mode and the counting rates for the two peaks were of the order of 10^6 cps. A calibration curve, based on analyses of olivine and orthopyroxene grains from Kilbourne Hole peridotite xenolith, 97-KH-6, was used. To assure direct comparison between laser ablation and solution nebulization analyses, the Fe/Mn ratios of olivines and orthopyroxenes from 97-KH-6 were analyzed by solution nebulization. Generally, the laser ablation technique used is free of matrix effects (Campbell and Humayun, 1999). The precision for standards and MORB glasses of the $^{57}Fe^+/^{55}Mn^+$ ratio by LA-ICP-MS was better than 1% (2σ).

3. RESULTS

It is important to observe that we have not attempted to precisely analyze either the Fe or Mn abundances in any of the samples, but that we directly determine the Fe/Mn ratio precisely. Abundances of MgO, FeO_{total} (FeO_T), and MnO were obtained from literature data for the same sample, where available. In several instances, the major-element abundances were determined by ICP-MS at the University of Chicago. We used our precise measurements of Fe/Mn and published (or measured) FeO_T to calculate MnO (MnO_C). These calculated MnO abundances are shown in Tables 1–4 and their precision and accuracy is controlled by the precision and accuracy of the FeO_T measurements.

3.1. MORB

Data for MORBs from the Pacific, Atlantic, and Indian oceans are given in Table 1 and shown in Fig. 2. Five of the freshest MORB samples from the Pacific (Juan De Fuca Ridge and East Pacific Rise) were analyzed by both SN-ICP-MS and LA-ICP-MS methods. The samples were leached following the procedures described above and the Fe/Mn in the leached residues are reported in Table 1, mean $Fe/Mn = 57.1 \pm 1.4$ (1σ). However, it was noted that although these samples had essentially no visible Fe–Mn oxide contamination the leached residues had higher Fe/Mn than LA-ICP-MS data, mean $Fe/Mn = 55.7 \pm 0.8$ (1σ). Further, the leachates were found to contain as much as 20% of the Fe, while Reinitz and Turekian (1989) reported only 0.2–2% sample loss for this leaching procedure. Accordingly, we combined data on the leachates and the residues to report a total Fe/Mn for each of these samples, as well (Table 1), mean $Fe/Mn = 56.5 \pm 1.1$ (1σ). These numbers are in better agreement with the LA-ICP-MS data, from which we conclude that the leaching procedure did more harm than good. All the MORB samples were analyzed by LA-ICP-MS and exhibited an Fe/Mn 53–56, a range of 5% (Table 1). The highest numbers (56) were observed systematically in Pacific MORB, and Fe/Mn correlates inversely with MgO indicating a control by

Table 1
Fe/Mn ratios by ICP-MS in MORB glasses from Pacific, Indian and Atlantic Oceans

Sample	MgO	FeO_T	MnO	Fe/Mn EMP	Fe/Mn SN	MnO_C SN	Fe/Mn LA	MnO_C LA
Pacific								
111240.0023	*6.93*	*11.75*	*0.20*	*58.97*	58.70[a]		56.23	0.210
					57.75[b]	0.204		
111240.0195	*6.67*	*11.36*	*0.20*	*57.01*	55.80[a]		55.95	0.204
					55.81[b]	0.204		
111240.0223	*6.85*	*11.68*	*0.19*	*61.70*	55.54[a]		56.20	0.209
					55.51[b]	0.211		
115200.0001	*9.33*	*9.34*	*0.16*	*58.59*	57.16[a]		54.30	0.173
	9.04	9.64						
					55.95[b]	0.168		
Alvin Dive 1376	*6.72*	*10.12*	*0.17*	*59.75*	58.06[a]		55.64	0.183
					57.61[b]	0.176		
115199	*15.14*	*9.74*	*0.17*	*57.50*			54.67	0.179
115739	*9.07*	*9.20*	*0.18*	*51.30*			54.28	0.170
	8.95	9.61						
Indian								
115290	9.65	7.71					53.13	0.146
115294.0012	8.29	9.45					54.39	0.174
115293.0002	7.98	9.31					54.32	0.172
VG6778	8.27	8.54					52.96	0.162
Atlantic								
115089.0084	7.30	10.19					53.92	0.190
113021.0071	7.25	10.02					54.39	0.185
115261	7.68	9.24					53.40	0.174

Major-element data sources: italicized values, this study; normal, Volcanic Glasses Project, Smithsonian Institution.
[a] Leached residues.
[b] Residue + leachate.

fractional crystallization. These numbers are lower than the leached MORB results reported in Humayun et al. (2004) for the same five Pacific MORB samples by 2.5%.

3.2. OIB (Iceland, Reunion, St. Helena, Tahiti)

Results for OIB from Iceland, Reunion, St. Helena, and Tahiti are given in Table 2. Except for ICE9 (Fe/Mn = 65.56), Fe/Mn ratios in all the Icelandic samples fall in the range of 58–62 (average Fe/Mn = 59.7 ± 1.8, 1σ), with MgO content varying from ~10–29% (Fig. 3). Fe/Mn is positively correlated with MgO content in these samples. Even the Icelandic picrites with the lowest MgO content have Fe/Mn ratios higher than those in MORB, resulting in a resolution of Iceland from MORB in Fe/Mn. Although we were careful to intercalibrate the two techniques used, inter-technique bias cannot be ruled out entirely to account for the offset between MORB and Icelandic picrites.

The single olivine basalt from Piton de la Fournaise (Reunion, Mascarene Islands, Indian Ocean) has a Fe/Mn = 65.65 at an MgO ~16% (Fig. 3a) compatible with Fe/Mn in picrites from Hawaii (Humayun et al., 2004). Its FeO (11.2; Fig. 3b) is comparable to Reunion lavas ($\sim 12 \pm 1\%$) reported by Albarede et al. (1997), and the MnO (0.171) is comparable to MnO in basalts from historic eruptions of Piton de la Fournaise (0.18 ± 0.01; Albarede et al., 1997), Hawaii (Humayun et al., 2004), and Iceland. Both Tahiti and St. Helena lavas have higher absolute MnO contents, in the latter case because these are more evolved lavas.

The three St. Helena samples exhibit a large variation in Fe/Mn ratios (47.35–63.42) within a narrow range of MgO content (~3–5%). Since these samples were all evolved, the results on these rocks are compared with previous data for St. Helena complied in GEOROC (Fig. 4a). MgO contents of St. Helena rocks vary from 16% to 0% in the GEOROC database. FeO_T contents are level at MgO >5% with a mean of 11.8 ± 0.8, but decrease at low MgO (high SiO_2). MnO contents are level at 0.18 ± 0.02 at MgO > 5%, but remain either constant or increase at low MgO (high SiO_2). Thus, the Fe/Mn ratio is level above MgO > 5%, but decreases dramatically at low MgO. The FeO_T and Fe/Mn ratios on the three St. Helena samples are compatible with this general trend. Basalts with higher MgO than those analyzed in the present study are needed to resolve St. Helena's Fe/Mn. The available XRF data for rocks with MgO > 5% provide a mean Fe/Mn = 65 ± 7, which spans the entire range of values observed by Humayun et al. (2004), and this study, from Hawaii to Iceland.

The seven Tahiti samples have higher Fe/Mn ratios (62.4–69.6) than most Icelandic samples, and overlap the Fe/Mn range obtained for Hawaiian picrites (Fig. 4b). There is more scatter in the seven samples than in equivalent suites from Hawaii. Some of this scatter may be due to post-eruptive weathering. Some of the scatter may be due to pooling samples from distinct volcanic centers, since we do not have the same level of information on these sam-

Table 2
Fe/Mn ratios by ICP-MS (SN) in ocean island basalts and USGS standards

Sample	MgO	FeO_T	MnO	Fe/Mn XRF	Fe/Mn SN	MnO_C SN
Iceland						
ICE0	20.11	9.02	0.160	56.56	56.66[a]	0.160
					58.18[b]	0.156
ICE2	20.72	8.41	0.147	57.44	56.09[a]	0.150
					58.81[b]	0.144
ICE3	18.00	11.11	0.186	59.97	61.15	0.182
ICE4A	25.27	9.89	0.164	60.52	61.32[a]	0.162
					61.44[b]	0.162
ICE4B	23.85	9.81	0.163	60.39	60.67	0.162
ICE5	18.76	9.64	0.164	58.98	59.90	0.162
ICE6	12.48	9.53	0.170	56.26	59.28	0.161
ICE8a	15.62	11.22	0.186	60.55	61.46	0.183
ICE8b	19.27	10.99	0.183	60.26	61.73	0.179
ICE9a	12.96	11.37	0.179	63.77	65.56	0.174
ICE10	12.33	9.52	0.168	56.87	58.77	0.163
ICE11	17.38	8.23	0.145	56.99	58.36	0.142
9805	28.47	8.37	0.139	60.42	61.12[a]	0.137
					61.64[b]	0.136
9806	15.17	8.28	0.146	56.91	58.13	0.143
9809	24.78	8.96	0.151	59.57	60.71[a]	0.148
					60.58[b]	0.148
9810	10.70	11.49	0.194	59.45	60.80[a]	0.190
					61.06[b]	0.189
9812	15.95	8.18	0.148	55.47	56.02	0.147
9815	9.47	10.76	0.187	57.76	58.53	0.185
DMF9101	22.37	9.73	0.164	59.53	60.36	0.162
				59.53	60.76	0.161
St. Helena						
109984	2.75	11.93	0.254		47.35	0.253
109982	4.68	12.53	0.212		59.47	0.211
109991	3.87	12.59	0.197		63.42	0.199
Tahiti						
100845	14.60	13.27	0.192		69.59	0.191
100899	20.72	13.18	0.189		68.76	0.192
100799	17.39	14.02	0.198		69.62	0.202
100783	12.76	12.23	0.199		62.38	0.197
100866	10.55	12.78	0.196		64.61	0.199
100842	8.04	12.18	0.185		66.87	0.183
100807	16.50	12.85	0.196		66.63	0.194
Reunion						
113259	15.72	11.20	0.169		65.65	0.171
USGS standards						
BHVO_2	7.23	11.07	0.167	66.69	65.93	0.169
BIR_1	9.70	10.17	0.175	58.32	59.54	0.171
BCR_1	3.46	12.06	0.180	67.23	65.67	0.184
BCR_2	3.59	12.42	0.196	63.50	62.00	0.201
DTS_1	49.59	7.81	0.120	65.33	60.91	0.129
PCC_1	43.18	7.51	0.120	62.84	64.01	0.118

Major-element data sources: Iceland (Brandon et al., 2007); St. Helena, Tahiti and Reunion (this study); USGS standards (USGS compilations).
[a] HF digestion.
[b] Carius tube + HF digestion.

ples as was available for Hawaii (Norman and Garcia, 1999). GEOROC data for ~90 volcanic rocks from the island of Tahiti with MgO > 5% indicate a constant $FeO_T \sim 12 \pm 1\%$. For lavas with MgO < 5% the FeO_T content of the lavas decreases with decreasing MgO, while the MnO content increases, so that Fe/Mn decreases. The Fe/Mn in GEOROC for samples with MgO > 5% has a high uncertainty, with average Fe/Mn ~ 69 ± 8 (1σ). By comparison, the 7 basalts analyzed here yielded a mean Fe/Mn = 67 ± 3 (1σ). The MnO concentrations obtained here yield a mean MnO = 0.194 ± 0.012 (2σ), much more precise than the GEOROC data which yield a mean

Table 3
Fe/Mn ratios by ICP-MS in komatiites

Sample	MgO	FeO_T	MnO	Fe/Mn XRF	Fe/Mn SN	MnO_C SN
Belingwe						
143.60–143.68	20.51				58.30	
144.60–144.70	27.49				58.48	
145.68–145.77	26.93				58.21	
148.02–148.12	28.63				58.68	
149.72–149.83	28.34				58.22	
ZV-10	26.21	10.21	0.17	60.29	58.07	0.176
Gorgona						
GOR 521	14.44	10.54	0.18		59.04	
Alexo						
ALX02	25.5	11.6	0.20	58.25	55.99	0.210
ALX04	24.6	11.4	0.20	57.35	57.83	0.200
ALX05	22.6	12.0	0.22	54.60	53.68	0.227
ALX07	23.7	11.2	0.21	53.76	53.98	0.212
ALX12	20.7	11.2	0.25	44.79	43.66	0.256
ALX14	25.8	10.9	0.18	60.71	60.48	0.183
ALX15	27.1	11.2	0.20	56.44	55.90	0.201
ALX16	33.9	9.90	0.16	62.09	61.56	0.164
ALX17	37.9	9.54	0.13	73.64	70.56	0.135
ALX18	39.7	9.00	0.12	75.26	76.02	0.119
ALX19	36.4	9.09	0.16	57.01	57.97	0.158
ALX20	35.4	9.45	0.15	63.22	65.48	0.143
ALX21	26.7	10.71	0.16	67.17	68.14	0.160
ALX20(ol)	50.16	8.39	0.132	63.79	60.20	0.139

Major-element data sources: Gorgona (Revillon et al., 2000); Alexo (Puchtel et al., 2004a); Belingwe (ZV-10 only, Nisbet et al., 1987).

Table 4
Fe/Mn ratios by ICP-MS in individual olivine and orthopyroxene grains separated from Kilbourne Hole xenolith, KH-97-6

Mineral Type	MgO	FeO_T	MnO	Fe/Mn SN	MnO_C SN
Olivine-1	50.57	9.28		69.68	0.134
Olivine-2	51.38	9.23		69.68	0.133
Olivine-3	52.18	9.39		69.78	0.135
Olivine-4	50.74	9.59		69.84	0.138
Olivine-5	48.80	9.28		70.16	0.133
Average $\pm 2\sigma_i$				69.83 ± 0.40	0.135 ± 0.004
Orthopyroxene-1	31.65	5.44		44.28	0.123
Orthopyroxene-2	32.27	5.64		44.37	0.128
Orthopyroxene-3	31.59	5.68		44.25	0.129
Orthopyroxene-4	32.20	5.65		44.15	0.128
Orthopyroxene-5	32.26	5.78		44.31	0.131
Average $\pm 2\sigma_i$				44.27 ± 0.16	0.128 ± 0.006

Major-element data source: this study.

MnO $\sim 0.17 \pm 0.06$ (2σ) after exclusion of several outliers. This demonstrates that a significant part of the Fe/Mn variability in the literature is due to imprecise MnO contents reported for volcanic rocks.

3.3. USGS standards

The Fe/Mn results for USGS standards (Table 2) are in good agreement (1–2%) with Fe/Mn ratios calculated from published compilations of FeO_T and MnO, with the exception of DTS-1 (differs by 7%). For the two ultramafic rocks, PCC-1 and DTS-1, the spinel residue was dissolved by carius tube digestion, and then combined with the stock solution. The BHVO-2 data plots along the Kilauea trend (Humayun et al., 2004). The BIR-1 datum is compatible with other Icelandic basalt data (e.g., 9815) reported in Table 2. The Fe/Mn of BCR-1 appears to be systematically higher than that of BCR-2 in both our dataset and the USGS compilations, for reasons that are unclear since BCR-1 and BCR-2 were sampled from the same flow. The MnO_c obtained from our precise Fe/Mn data and the MnO from the compiled data agree to 1–2%, with the

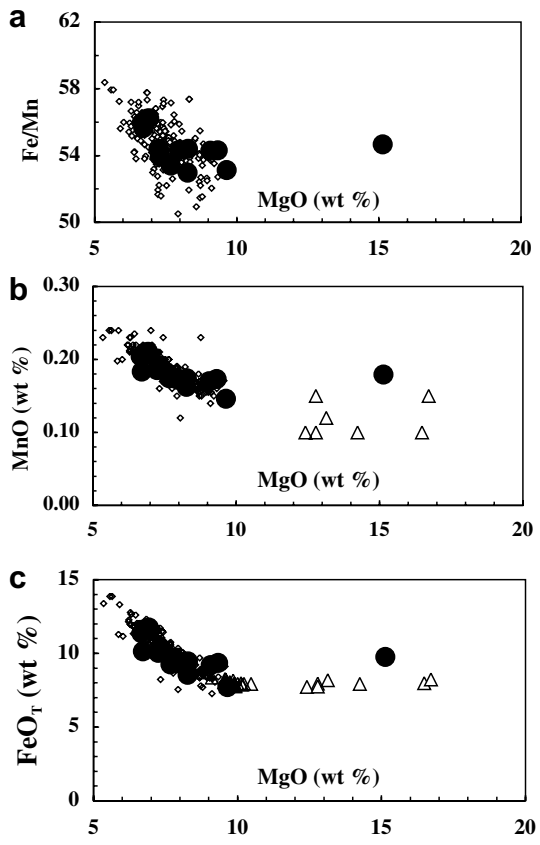

Fig. 2. Comparison of MORB data from this study (solid circles) with LDEO DCP data (small gray diamonds; PETDB). (a) Fe/Mn ratio vs. MgO; (b) MnO vs. MgO; (c) FeO_T vs. MgO, including MORB picrites from the Siqueiros Fracture Zone (open triangles; Perfit et al., 1996). Note, the similarity of values measured in this study with DCP data. Also, the effect of fractionation increases FeO_T, MnO and Fe/Mn, but while FeO_T increases by nearly a factor of two, Fe/Mn increases by 6%.

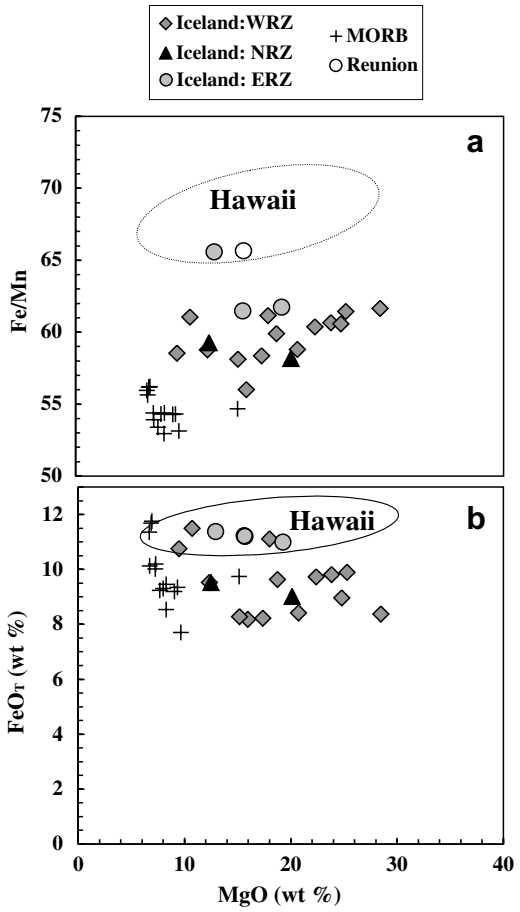

Fig. 3. Icelandic picrites and basalts from each of the three major rift zones, and the single Reunion picrite: (a) Fe/Mn, and (b) FeO_T vs. MgO (same *x*-axis scale). Field for Hawaiian picrites (Humayun et al., 2004) and data for MORB (this study) are shown for comparison. The Reunion picrite in (b) is buried under an Iceland picrite with identical MgO and FeO_T.

exception of DTS-1 (which differs by 7%). We suspect that the 7% difference between our Fe/Mn for DTS-1 and the compiled value is due to underestimation of the MnO abundance in the USGS compilation.

3.4. Komatiites

Komatiite Fe/Mn ratios are given in Table 3. Although komatiite flows exhibit strong internal differentiation, the Fe/Mn ratio remains constant ($58.33 \pm 0.8\%$) among the six Belingwe samples, with MgO content varying between ~20% and 29% (Fig. 5). The Fe/Mn of 58.33 is close to those for Iceland samples. The single Gorgona Island komatiite analyzed (GOR 521) has a Fe/Mn ratio of 59. Alexo samples exhibit a large range of Fe/Mn that we attribute to post-magmatic alteration. The olivine-rich cumulates appear to have lost Mn during serpentinization.

3.5. Individual mineral grains from a Kilbourne hole xenolith

Five olivine and five orthopyroxene grains from a single Kilbourne Hole peridotite, KH-97-6, were analyzed for Fe/Mn (Table 4) to examine the reproducibility of the technique. Our Fe/Mn results are identical to the individual olivine and orthopyroxene analyses for a Kilbourne Hole xenolith obtained by electron microprobe analysis (Dyar et al., 1992), except for better precision. In the present study, the five olivine crystals and five orthopyroxene crystals have uniform Fe/Mn ratio of 69.83 ± 0.40 (2σ) and 44.27 ± 0.16 (2σ), respectively, (Fig. 6). The external reproducibility for olivine grains is better than 0.6%, and for orthopyroxene is better than 0.4%. This showed that the KH-97-6 olivines and orthopyroxenes were very homogeneous from grain-to-grain. Further, olivines exhibit a systematically higher Fe/Mn than orthopyroxenes, as also seen in experimental partitioning coefficients at higher equilibration temperatures (Walter, 1998; Humayun et al., 2004).

3.6. The effect of incomplete dissolution on Fe/Mn

Picrites and komatiites contain chromite-spinel minerals that are insoluble in HF/HNO_3 at hotplate temperatures.

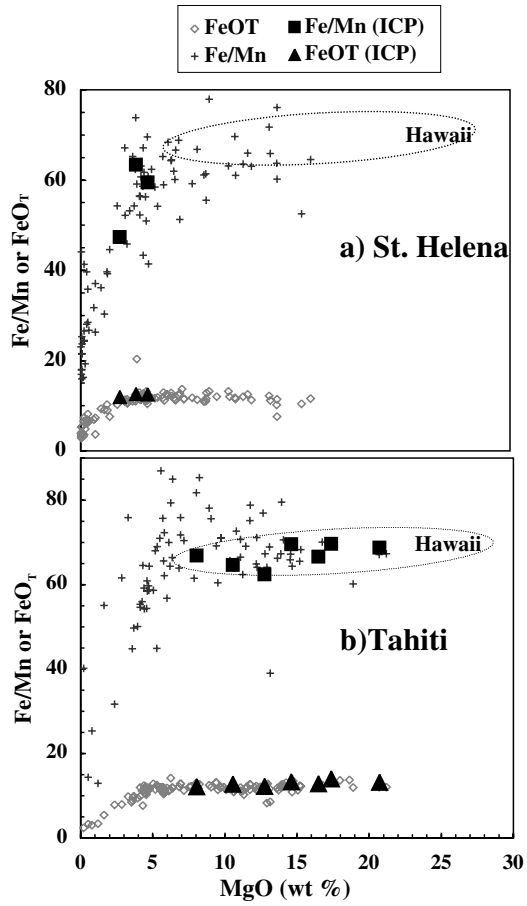

Fig. 4. Plots of Fe/Mn and FeO_T for (a) St. Helena; and (b) Tahiti lavas. Literature Fe/Mn data are shown as crosses and literature FeO_T data are shown as gray diamonds (sources GEOROC). Field for Hawaiian picrites shown as an ellipse.

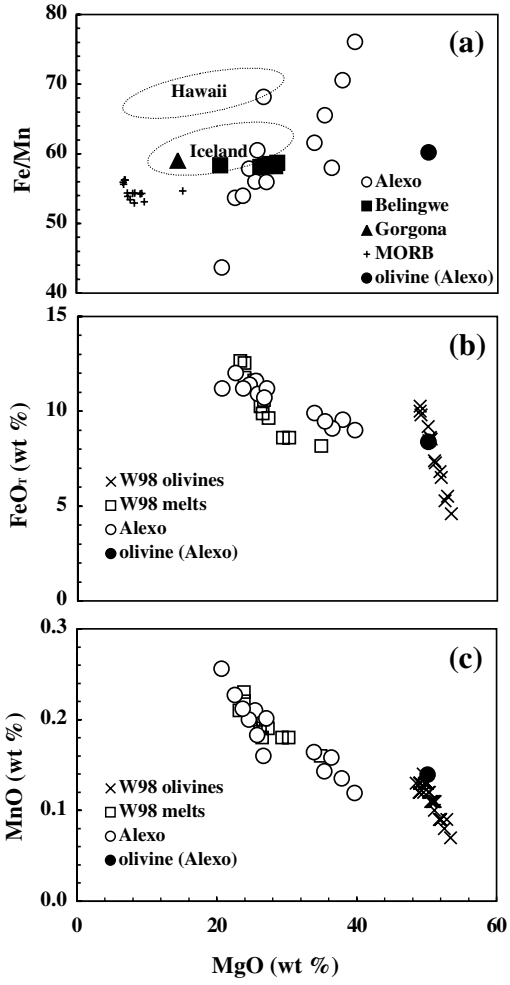

Fig. 5. Plot of (a) Fe/Mn vs. MgO for komatiites, with Hawaiian and Icelandic Fe/Mn ranges shown as ellipses, and MORB plotted as black crosses. Note the large range of Alexo Fe/Mn due to alteration, while the single Alexo olivine plots in line with Belingwe and Gorgona data. Separate plots of (b) FeO_T vs. MgO, and (c) MnO vs. MgO (all panels on the same scale) for Alexo komatiites. Experimental melts and residual olivines from Walter (1998) shown for comparison.

The effect of incomplete dissolution of these minerals on the measured Fe/Mn ratio was examined by comparing six Iceland picrites by both carius tube digestion and hotplate acid digestion. The results are given in Table 2. The two methods reproduce the Fe/Mn ratio to better than 1% with two exceptions, Ice 0 and Ice 2, where the Fe/Mn obtained by CT + HF is higher by 3–5%. The higher values obtained by carius tube digestion are more in line with the trend of Fe/Mn vs. MgO for Reykjanes picrites, and have been adopted here.

4. DISCUSSION

4.1. Fractional crystallization

Relating erupted liquid Fe/Mn ratios to source Fe/Mn ratios requires knowledge of the effect of fractional crystallization and partial melting processes on the liquid's Fe/Mn ratio. The FeO_T of the primitive liquid is also of interest, here. A large database of analyses of major-element compositions for both MORBs (PETDB) and OIBs (GEOROC) is available upon which we have drawn to augment our limited FeO_T data. We have used correlations between FeO_T and MgO to estimate primitive liquid compositions. The present data do not constrain the exact value of Fe/Mn in the mantle sources, since the fractionation that occurs upon melting is not fully known. Fe/Mn ratios in peridotites indicate that MORB and Icelandic basalts have Fe/Mn ratios about 10% lower than fertile Kilbourne Hole peridotites, while lavas from Hawaii, Tahiti, and Reunion have Fe/Mn ratios about 10% higher than fertile Kilbourne Hole peridotites (Humayun et al., 2005).

MORBs are strongly fractionated by removal of olivine, plagioclase and clinopyroxene (Bryan, 1983). Olivine removal decreases Fe/Mn and (for Fo < 87) decreases FeO_T. Plagioclase removal has a negligible effect on Fe/Mn but will increase FeO_T. Clinopyroxene removal will increase Fe/Mn and FeO_T. A dataset of about 280 MORB analyses selected from the PETDB database, all analyzed by Direct Current Plasma (DCP) in the laboratory of Charlie Lang-

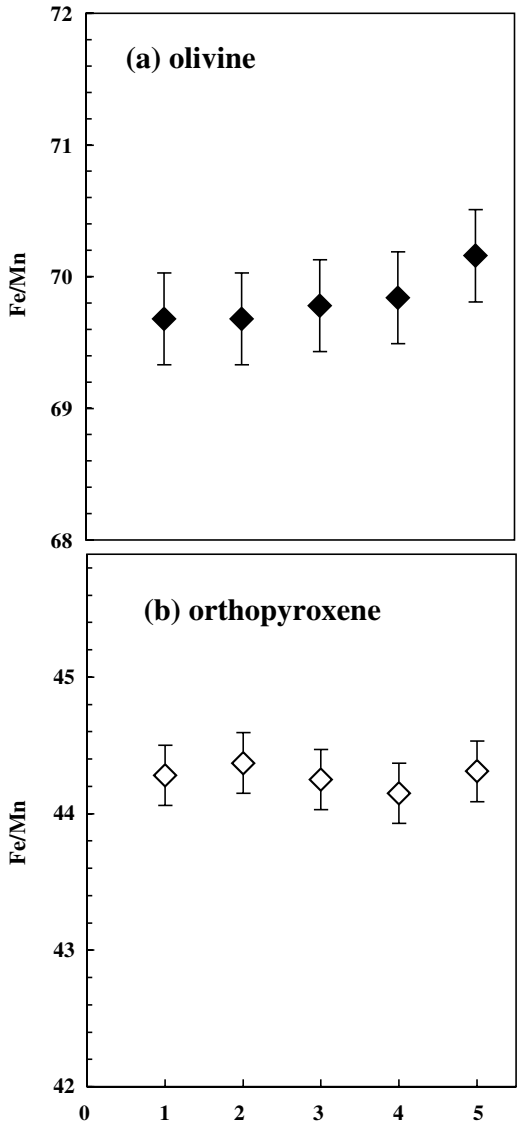

Fig. 6. Five replicate analyses Fe/Mn in (a) olivine, and (b) orthopyroxene, from a single Kilbourne Hole xenolith. Note the different vertical scales and the excellent reproducibility of the measurements.

muir at LDEO, is shown for comparison in Fig. 2. These analyses have Fe/Mn ratios comparable in precision to the laser ablation ICP-MS analyses reported in this study. For MORBs with MgO > 5%, the Fe/Mn ratio and FeO_T increase with decreasing MgO in a consistent way (Fig. 2a and b). The analyses reported here overlap the LDEO DCP data, with the exception of the magnesian basalt (#115199, MgO = 15.14%) which has an Fe/Mn = 54.67. The highest FeO_T and Fe/Mn ratios are observed in Pacific MORB (Table 1), presumably because Pacific MORB are systematically more fractionated than Atlantic and Indian MORB. To augment the MORB data at MgO > 10%, MORB whole rock and glass analyses from the Siqueiros Fracture Zone (Perfit et al., 1996) are plotted in Fig. 2b. Using the trend of FeO_T vs. MgO, we obtain $FeO_T \sim 9.7\%$ at MgO = 8% and $FeO_T \sim 8.0 \pm 0.2\%$ (1σ) at MgO $\geqslant$ 10%, the latter value identical to that obtained by Putirka (2005) from the same dataset. The lowest MORB Fe/Mn ratio at MgO $\sim$ 10% is 53, increasing at both lower and higher MgO contents. Klein and Langmuir (1987) estimated primitive MORB liquids to have MgO = 10–15%., so that Fe/Mn in primitive MORB is constrained to be 54 ± 1, but our coverage of Fe/Mn in MORBs at MgO > 10% is limited to a single analysis. A straight average of Fe/Mn ratios for all MORB data with MgO > 7% from this study yields a ratio of 54.0 ± 1.2 (2σ), which will be used to represent primitive MORB in subsequent discussion. The increase in liquid FeO_T from MORB with MgO > 10% (8.0 ± 0.2, 1σ) to Hawaii (11.4 ± 0.3, 1σ; Putirka, 2005) is consistent with petrological interpretations of a higher FeO_T in mantle melts derived from greater depths (Langmuir and Hanson, 1980; Albarede, 1992).

Fractionation of primitive MORB may follow along an olivine control line that decreases Fe/Mn with decreasing MgO, as it does in most observed OIB lava suites (Humayun et al., 2004; this study). However, at MgO < 8% MORB basalts exhibit increasing Fe/Mn with decreasing MgO, indicating that a crystallizing phase is removing Mn. The likely phase is clinopyroxene (augite) and implies that clinopyroxene may play an important role in shallow-level MORB fractionation (e.g., Bryan, 1983; Grove and Bryan, 1983).

Icelandic picrites and basalts from all three major rift zones were sampled and powdered for Os and He isotope analyses by Brandon et al. (2007) and we follow their nomenclature, below. Picrites from the Reykjanes ridge and Western Rift Zone (WRZ) and from the Northern Rift Zone (NRZ) have systematically lower Fe/Mn and FeO_T than Hawaiian shield lavas (Fig. 3). Picrites from Skirdufell, in the Eastern Rift Zone (ERZ), and some lavas from the WRZ, have FeO_T similar to those of Hawaiian lavas, and higher than other Icelandic lavas (Fig. 3). The ERZ lavas (MgO 13–19%) have $FeO_T = 11.2$, and Fe/Mn = 61.5-65.6, intermediate between Hawaiian lavas and lavas from other parts of Iceland. The origin of the higher Fe/Mn in ERZ lavas is unclear at present, and is controlled by the high Fe/Mn in Ice 9a (Table 2). With the present dataset, distinctions among groups from WRZ and NRZ are hard to recognize, which all yield $FeO_T \sim 9$–10, and a Fe/Mn = 59.6 ± 1.6. The WRZ picrites represent many individual volcanoes and so do not define clear fractionation trends with MgO. Several of the highest FeO samples from the WRZ are basalts (9810, 9815; Brandon et al., 2007) and have evolved from olivine fractionation towards clinopyroxene fractionation, which would tend to increase their Fe/Mn ratio. This effect has not been noted in Kilauea lavas >7% MgO (Humayun et al., 2004). The WRZ picrites have higher Fe/Mn than MORB which includes uncorrected fractional crystallization effects.

The single sample from Piton de la Fournaise volcano (Reunion, Mascarene Islands, Indian Ocean) has an MgO $\sim$ 16, which is intermediate between two clumps of Reunion data observed by Albarede et al. (1997). Reunion yields a $FeO_T = 11.4 \pm 0.5$ at 15% MgO from a regression

of analyses from Albarede et al. (1997), and a Fe/Mn ratio of 65.7 from our single analysis (Table 2). The primitive liquid for Reunion is estimated to have an MgO ~ 15 (Albarede et al., 1997), so that fractionation correction to the measured value is negligible. The Reunion value compares well with the Fe/Mn calculated from XRF data on historic lavas from Piton de la Fournaise (Albarede et al., 1997), which also overlap the Fe/Mn range for Hawaiian lavas, and are systematically higher than Icelandic lavas and MORB (Fig. 3).

For St. Helena, Fig. 4a shows Fe/Mn ratios and FeO_T vs. MgO from literature sources and data from Table 2. The FeO_T is relatively constant at MgO > 5%, but declines rapidly at lower MgO. The MnO is relatively constant at MgO > 5%, but increases at lower MgO. Thus, the Fe/Mn ratio is relatively constant at MgO > 5%, but decreases at lower MgO. Our three St. Helena samples were all classified as basalts, but had MgO < 5%. A $FeO_T \sim 11.8$ is estimated for primitive liquids from the GEOROC database, but the Fe/Mn is not well constrained from the database. An average Fe/Mn of the two samples with highest Fe/Mn (Table 2) yields 62 ± 3. Better characterization of the Fe/Mn of St. Helena samples with MgO > 5% is needed.

Basalts from Tahiti (Fig. 4b) exhibit a similar behavior as those from St. Helena, with a mean $FeO_T = 12 \pm 1$ (for MgO > 5%) and a mean Fe/Mn = 67 ± 3, in the same range as the Hawaiian lavas (Humayun et al., 2004). The higher FeO_T obtained is similar to that obtained by Albarede (1992) for the Tahiti 1 group. Six of the seven analyzed basalts have olivine phenocrysts, and MgO 8–20%, comparable to the Hawaiian (Humayun et al., 2004) and Icelandic lavas. Thus, lavas from Tahiti, Reunion and Hawaii exhibit systematically higher Fe/Mn > 65; Icelandic picrites (and the limited St. Helena basalts) exhibit lower Fe/Mn ~ 58–61; while MORBs form a distinct group with Fe/Mn ~ 54. This is a total range of variation of Fe/Mn of 20–25%. To consider the effects of partial melting, particularly the depth of melting, in controlling FeO_T and Fe/Mn we examine high pressure experimental melting of peridotite, in a subsequent section.

4.2. Fe/Mn in komatiites

The Fe/Mn vs. MgO for komatiites is shown in Fig. 5. Belingwe komatiites (2.7 Ga) were reported to have radiogenic initial $^{187}Os/^{188}Os$ ratios (Walker and Nisbet, 2002), similar to that of the 2.8 Ga Kostomuksha komatiites (Puchtel et al., 2005). However, new Os isotope results for the Belingwe komatiites indicate unradiogenic initial $^{186}Os/^{188}Os$ and $^{187}Os/^{188}Os$ ratios (Puchtel et al., 2007) identical to that of the Abitibi komatiites (Puchtel et al., 2004b). Because the Kostomuksha komatiites are metamorphosed we did not attempt to analyze these for Fe/Mn ratios, but the Belingwe komatiites have experienced very low level metamorphism (Nisbet et al., 1987). Gorgona komatiites (90 Ma) exhibit correlated radiogenic $^{186}Os/^{188}Os$ and $^{187}Os/^{188}Os$ ratios (Brandon et al., 2003), and a single sample (GOR 521) was analyzed for its Fe/Mn ratio. Both the Gorgona komatiite (GOR 521) and the Belingwe komatiites exhibit uniform Fe/Mn ratios of 59.0 and 58.3 ± 0.2 (1σ) with no correlation between Fe/Mn and MgO. For Belingwe samples, Fe/Mn remains constant in all the samples from the olivine spinifex to olivine accumulate zone of Onias's flow and Tonys's flow (see Nisbet et al., 1987, for a discussion of these flows). This Fe/Mn is higher than MORB determined by LA-ICP-MS but overlaps the range of Iceland picrites. The Belingwe komatiites do not appear to have originated from a high Fe/Mn source. The single Gorgona analysis does not provide particularly firm constraints on the Fe/Mn of the Gorgona plume source, but it is noteworthy that none of the Hawaiian picrites exhibit a similarly low Fe/Mn. The radiogenic $^{187}Os/^{188}Os$ (0.138024) and $^{186}Os/^{188}Os$ (0.1198452) obtained in GOR 521 was taken as evidence of core–mantle interaction (Brandon et al., 2003). Thus, a correlation between radiogenic $^{186}Os/^{188}Os$ (or $^{187}Os/^{188}Os$) and high Fe/Mn is not supported by these data for this Gorgona komatiite, although we caution here that a single analysis might be misleading.

The Fe/Mn ratio of Alexo komatiites shows a very large range, 44–76 (Fig. 5a), for igneous rocks originating by flow differentiation. This is very likely the result of the redistribution of Fe and Mn during hydrothermal alteration and metamorphism in the Alexo area (Lahaye et al., 1995; Lahaye and Arndt, 1996). An olivine mineral separate from ALX20 (Puchtel et al., 2004a) has an Fe/Mn ratio of 60.2 (Table 3). This value is lower than estimated for olivines from Hawaii (Fe/Mn > 70), or olivine from the Kilbourne Hole xenolith (Fe/Mn ~ 70). Both the FeO and MnO contents of olivine decrease with increasing MgO content (temperature) of the liquid (Fig. 5b and c), and the low Fe/Mn of ALX20 olivine implies that Fe/Mn in olivine also decreases with increasing temperature. The expectation for the Alexo flows is that primary FeO_T and MnO abundances should plot on olivine control lines. The ALX20 olivine separate defines the position of magmatic olivine in a cumulate komatiite, while the spinifex komatiites define the liquid end-member (Fig. 5b and c). To establish whether the spinifex komatiite compositions are close to primary melt compositions in terms of their FeO_T and MnO, the 6–7 GPa experimental melts from Walter (1998) are shown for comparison in Fig. 5b and c. The spinifex komatiites plot close to the experimental melts in both FeO_T (Fig. 5b) and MnO (Fig. 5c). The ALX20 olivine plots on the line of residual olivine compositions from 6 to 7 GPa experiments (Walter, 1998). The olivine cumulate portion of the Alexo flows, i.e., with MgO from 34% to 40% shows a systematic depletion in MnO (Fig. 5c), likely caused by MnO loss during serpentinization of olivine. A smaller depletion in FeO_T is also possible (Fig. 5b), with the net result that Fe/Mn in the cumulate portion is very high (Fig. 5a). While the olivine cumulate portions of the Alexo flow lost MnO, at least one sample (ALX12) in the upper portion of the flow appears to have gained MnO. Two spinifex komatiites (ALX 02, ALX 04) from the A_2 zone of the Alexo flow (Puchtel et al., 2004a) have Fe/Mn ~ 57, just slightly lower than the GOR521 and Belingwe komatiites, which may be the closest samples to magmatic compositions based on their texture, degree of preservation (Puchtel et al., 2004a), and their FeO_T and MnO abundances.

4.3. Depth and degree of melting

Albarede (1992) observed that FeO_T in OIB melts, when corrected to 15% MgO for the effects of fractionation, could be used as an indicator of depth and degree of melting. In general, FeO_T is better determined than MnO in igneous rocks and experimental studies, so we will consider FeO_T and Fe/Mn in experimental melts to constrain the role of pressure in determining the Fe/Mn variations in lavas. Its worth noting the caveat here that the Fe/Mn ratios obtained from experimental melts are of lower precision than the measurements we are trying to interpret. However, the experimental data provide constraints that are valuable for interpreting the coarsest scale of Fe/Mn variation observed here, a difference in Fe/Mn of ~25%. Fig. 7 shows FeO_T vs. MgO for experimental melts produced at 3–7 GPa from the study of Walter (1998) and at 1 GPa from Hirschmann et al. (1998) and Pickering-Witter and Johnston (2000). All three studies used fertile lherzolites for their starting materials. Additionally, Pickering-Witter and Johnston (2000) explored the effect of variable source mineralogy. Melts from their compositions FER-B, FER-D and FER-E are shown in Fig. 7; melts from their composition FER-C (opx-dominated) have a steeper slope (not shown in Fig. 7). In Fig. 7, it can be observed that the FeO_T of low- to moderate-degree (<15%) partial melts of fertile lherzolite increases from about 6% (at 1 GPa) to about 12% (at 7 GPa) with increasing pressure. At constant pressure (isobaric melting), the FeO_T decreases with increasing degree of partial melting (increasing T) at $P > 3$ GPa (Walter, 1998), but the opposite effect is seen at 1 GPa (Hirschmann et al., 1998; Pickering-Witter and Johnston, 2000; Stolper et al., 2004). The results of Pickering-Witter and Johnston (2000) show that increasing the cpx/opx ratio in the source produces melts with FeO_T steady at about 6.2–6.8% at 1 GPa. Superposed on the experimental melt composition curves are estimates of the mean FeO_T at ~15% MgO (termed FeO_{15}) for each of the OIB localities studied here, and for MORB at 10% MgO. At 10% MgO MORBs have $FeO_T \sim 8.0\%$ which require pooling melts from 1 GPa with melts derived from higher pressures (>3 GPa). By comparison, Icelandic picrites and basalts from the northern and western rift zones, including Theistareykir and Reykjanes Peninsula, have FeO_{15} about 9–10%. Picrites from the Eastern Rift Zone (Ice 8a,b and 9) have higher $FeO_{15} \sim 11\%$. These lavas are closer in FeO_T to lavas from Kilauea, Mauna Loa, St. Helena and Reunion. Lavas from Tahiti have a $FeO_{15} \sim 12$, representing either lower degree partial melts or deeper melts. Albarede (1992) estimated the FeO_T for primitive melt compositions from several OIB localities and obtained results very similar to those obtained here. Albarede (1992) assumed that, to first order, major-element heterogeneities in the mantle could be ignored and then adjusted these primary melt compositions to be in equilibrium with Fo91 olivine. Examples of some of his results for the same OIB localities are shown for comparison in Fig. 7. Since the premise of the present study is that FeO_T may be variable in the source regions of OIB, we did not adjust our estimated melt compositions to be in equilibrium with a specific olivine composition. The only significant difference between the estimated primary melt compositions of Albarede (1992) and this study are in the MgO content, largely due to the Fo91 correction applied by Albarede (1992).

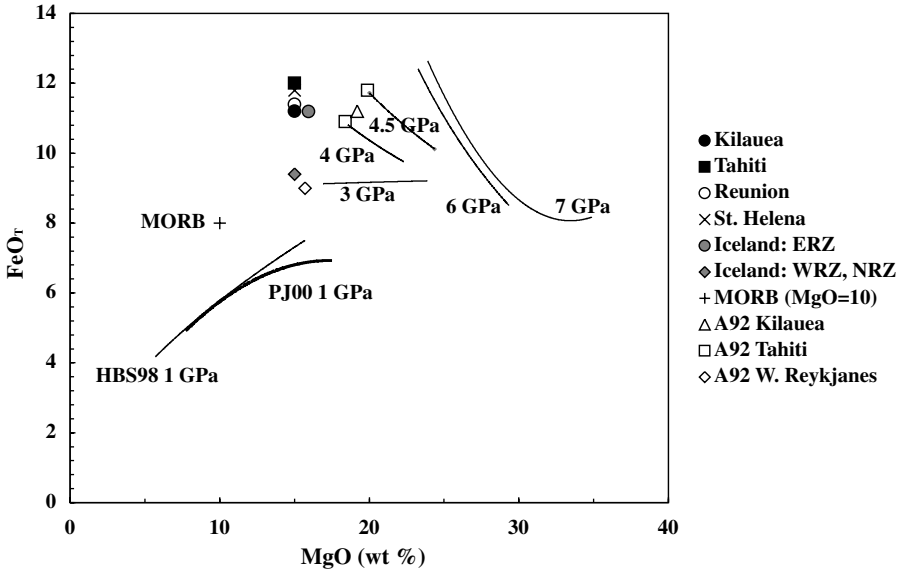

Fig. 7. A comparison of FeO_T vs. MgO for experimental melts from fertile peridotites in the pressure range 1 to 7 GPa with fractionation corrected FeO_T at 10% MgO for MORB and 15% MgO for OIB localities in this study. Also included are estimates of parental liquid compositions from Albarede (1992, A92). The trends in the experimental melts are shown as best-fit curves to the data of Hirschmann et al. (1998, HBS98) and Pickering-Witter and Johnston (2000, PJ00) for 1 GPa, and to Walter (1998) for 3–7 GPa. Note, that Iceland is shown as gray diamonds (WRZ, NRZ) and as gray circles (ERZ). The gray circles have been offset at 16% MgO for purposes of display. The MORB data are shown at 10% MgO.

The pressure effect on melting contributes a change of over a factor of two in FeO content from ~6 wt% FeO at 1 GPa to ~12 wt% FeO at 7 GPa (Fig. 7). The variation in FeO_T for primary melts ranges from 8 wt% FeO_T (MORB) to 12 wt% FeO_T (Tahiti) (Fig. 7), a range of 50% relative change in FeO_T. Although 6 Icelandic picrites and basalts exhibit the same high FeO_T as Hawaiian lavas, only one of those picrites has an Fe/Mn comparable to the Hawaiian lavas (Fig. 3a). Higher FeO_T in these 5 Icelandic lavas must be accompanied by higher MnO to yield a constant Fe/Mn ratio in these lavas. In such instances, high FeO_T may be a function of depth of melting alone (Albarede, 1992). However, a subset of OIB studied here from Hawaii, Tahiti, and Reunion, have similarly high FeO_T to the highest FeO_T Icelandic lavas, but also have higher Fe/Mn ratios. It is the origin of this Fe/Mn variability that was attributed to possible core–mantle interaction by Humayun et al. (2004), and will be discussed further in Section 4.4.

4.4. Origin of global variability in Fe/Mn for hotspots

Our present data extend the observation of Humayun et al. (2004) on Hawaii to include Tahiti, and possibly Reunion, among hotspots that exhibit high Fe/Mn. Courtillot et al. (2003) classified hotspots into three types: primary hotspots originating from the D" region at the core–mantle boundary, including Hawaii, Reunion and Iceland; secondary hotspots originating above mantle superswells identified by seismic tomography, including Tahiti; and tertiary hotspots possibly originating in the asthenosphere, including St. Helena. Niu et al. (2002) provide seismic evidence for a deep (>660 km) mantle plume beneath the Society islands. Montelli et al. (2004) provided tomographic evidence that Tahiti may be rooted at the core–mantle boundary so the elevated Fe/Mn may also have resulted from the interaction between the outer core and lower mantle at the boundary layer. Jellinek and Manga (2004) argued for links between long-lived hotspots and the CMB. The present distribution of high Fe/Mn plumes recognized in this study coincides with plumes with ultra-low velocity zones at the CMB (Jellinek and Manga, 2004).

The seismic evidence on the depth of origin of the well-studied Iceland plume is ambiguous. Bijwaard and Spakman (1999) noted seismic evidence of CMB structure beneath Iceland. Wolfe et al. (1997) argued for a plume above 660 km, but lacked the resolution to image the plume any deeper than that. Shen et al. (2003) interpreted seismic velocity discontinuities at 1050 km beneath Iceland as evidence of a deeper plume. Montelli et al. (2004) resolved only a shallow plume beneath Iceland while, in a subsequent study, Montelli et al. (2004) proposed a pulsating plume possibly extending to the core–mantle boundary. We did not find evidence of high Fe/Mn in the majority of Icelandic lavas. This is corroborated by the lack of radiogenic $^{186}Os/^{188}Os$ in the same lavas (Brandon et al., 2007).

As argued by Humayun et al. (2004), the Fe/Mn ratio is better determined by mass spectrometry than the individual elemental abundances. An increase in Fe/Mn can then be caused by an increase in the FeO of the melt, or by a decrease in the MnO of the melt. Discriminating between these two choices is not possible at the level of the observed signal, ~24% relative increase in the Fe/Mn ratio. Consider that among the OIB lavas which show high Fe/Mn, Tahiti has an FeO_T about 10% relative higher than Kilauea, but essentially the same Fe/Mn. Variability in the FeO_T values for different OIB is not uniquely linked to their Fe/Mn (Fig. 7) indicating that factors such as depth of partial melting contribute importantly to their FeO_T (as proposed by Albarede, 1992).

Sobolev et al. (2005) have proposed that Hawaiian shield lavas may originate from mantle sources entirely devoid of olivine and that this might account for their higher Fe/Mn. Humayun et al. (2004) observed that the similar compatibilities of Fe and Mn in mantle-derived melts was based on a balance between olivine (high Fe/Mn phase) and pyroxene + garnet (low Fe/Mn phases). If an olivine-free source for Hawaii indeed turns out to be correct, it potentially could explain the elevated Fe/Mn in Hawaiian lavas since our arguments, and those of Humayun et al. (2004), are based on experimental melting studies of olivine-dominated peridotitic sources. This would then imply that all high Fe/Mn lavas originated from source regions that had been significantly modified from a peridotite source. Sobolev et al. (2007) extended the conclusions of Sobolev et al. (2005) to include global MORB and OIB. They argued that the effect of secondary pyroxenites on the melt compositions of erupted lavas was related to the depth of melt extraction: negligible in MORB, slightly evident in Iceland and strongest in intraplate plumes like Hawaii and Tahiti. Sobolev et al. (2007) found that Fe/Mn in olivines increased in the order MORB < Within-Plate Magmas on lithosphere <70 km thick (WPM-thin; e.g., Iceland) < Within-Plate Magmas erupted on lithosphere >70 km thick (WPM-thick, e.g., Hawaii, Reunion, Tahiti), which is qualitatively in accord with the results of this study. In the present study, MORB are resolved from Icelandic picrites and komatiites, while the latter two are unresolved from each other in Fe/Mn ratios. Huang et al. (2007) tested the Sobolev et al. (2005, 2007) hypothesis that the contributions of secondary pyroxenites were highest in the source of Ko'olau lavas and lower in the sources of Kilauea and Loihi lavas by measuring Fe/Mn ratios in Ko'olau lavas, and found that Ko'olau lavas exhibit the same Fe/Mn ratios as other Hawaiian lavas (Humayun et al., 2004). Their result is inconsistent with the prediction by Sobolev et al. (2007) of enhanced effect of secondary pyroxenite in the Ko'olau source region, relative to Kilauea. A global test of the Sobolev et al. (2005, 2007) hypothesis is required.

Another possible cause of Fe/Mn variability is mantle source redox variations. Based on the work of Canil et al. (1994), ferric iron (Fe^{+3}) is more incompatible than ferrous iron (Fe^{+2}), leading to higher Fe/Mn in lavas formed by the melting of more oxidized sources. [As a caveat, it should be noted that Bezos and Humler (2005) found no variations of $Fe^{+3}/\Sigma Fe$ as a function of degree of melting in MORBs, contrary to the expectation that ferric Fe is more incompatible.] Redox states of iron are known for MORB lavas (Bezos and Humler, 2005) and Mauna Loa lavas (Rhodes and Vollinger, 2005). Rhodes and Vollinger (2005) found that lavas from the historic 1984 Mauna Loa eruption collected directly from the vent had $Fe^{+3}/\Sigma Fe = 0.082 \pm 0.014$ (1σ),

while lavas collected from flows further from the vent were more oxidized with $Fe^{+3}/\Sigma Fe$ ratios of 0.09–0.28. The vent $Fe^{+3}/\Sigma Fe$ numbers, which were considered to be representative of the pre-eruptive $Fe^{+3}/\Sigma Fe$ ratios, are slightly more reduced than recent MORB measurements ($Fe^{+3}/\Sigma Fe = 0.12 \pm 0.02$ (1σ), Bezos and Humler, 2005). The Fe/Mn ratios for Mauna Loa picrites (~66, Humayun et al., 2004), like other Hawaiian lavas, are higher than MORB (~54, this study) rather than lower, the opposite of what would be expected from source redox differences as the cause of Fe/Mn variations. It should be appreciated that post-eruptive oxidation can increase the $Fe^{+3}/\Sigma Fe$ of lavas, but will not affect the Fe/Mn ratio.

Other possibilities that have been raised include speculations about a Fe-rich residual liquids remaining after a Hadean magma ocean (Lee et al., 2007) and melt extraction from refractory harzburgites to obtain high Fe/Mn (Lee, 2004). The role of refractory harzburgites was shown to be ineffective in controlling the Fe/Mn in melts since the increase in the olivine modal fraction increases the bulk Fe/Mn but also increases the bulk D for FeO (Humayun et al., 2005). If a Hadean magma ocean left behind a Fe-rich layer in the deep mantle and this layer is still preserved, it could potentially explain the high Fe/Mn ratios observed in some OIB (Lee et al., 2007).

For peridotite sources, the elevated Fe/Mn requires an origin from an Fe-rich peridotite. We are then left asking the question: what factors could vary mantle source MnO or FeO_T abundances? There are no known global reservoirs of high MnO material available for decreasing the Fe/Mn ratio of MORBs and OIBs relative to Hawaii, with the possible exception of Mn-sediments (Ravizza et al., 2001). A more sensitive measure of the amount of Mn-sediments in the sources of Hawaiian basalts than Fe/Mn ratios appears to be the abundance and isotopic composition of Tl. Nielsen et al. (2006) showed from the presence of correlated δ^{203}Tl vs. Cs/Tl ratio that the amount of Mn crust present in the source of Hawaii is too small to explain the radiogenic Os isotopic composition (Brandon et al., 1998, 1999) or affect its elevated Fe/Mn ratios (Humayun et al., 2004). That leaves a source of high FeO. The obvious source for this is the Earth's liquid outer core. Whether the outer core is a source (Rubie et al., 2004) or a sink (Takafuji et al., 2005) for FeO depends critically on the solubility of oxygen in the core (Humayun et al., 2004). Recent experimental studies of the Fe-solubility in the post-perovskite phase show that it can accommodate over 40 mol% $FeSiO_3$, and that this could explain seismic observations of ultra-low velocity zones at the core–mantle boundary (Mao et al., 2006). A lot remains to be learned about the nature of core–mantle boundary exchange and its link to high Fe/Mn mantle sources for OIB lavas.

4.5. Elemental signatures of core–mantle interaction

Here we consider the possible impacts of core–mantle interaction on elements other than Fe and Mn as a discriminatory test for core–mantle interaction. Sobolev et al. (2005) observed that Ni contents and Fe/Mn ratios of olivines from Hawaiian basalts were systematically higher than those from many other localities. They rejected the possibility that core–mantle interaction could explain the higher Ni contents because this would require about 3% outer core addition to the sources of Hawaiian lavas, which is higher than estimated from Os isotopes (⩽1%; Brandon et al., 1999). They argued that "any input from the core should markedly increase the platinum group element abundances in the Hawaiian source and melts" which "could be suppressed in the melts only by an exceptionally large amount of residual sulphides". These arguments are based on the assumption that outer core liquid is simply added to the mantle source region without consideration of the effects of elemental partitioning. Bennett et al. (2000) showed that abundances of platinum group elements (PGEs) are not enhanced in the same Hawaiian picrites analyzed for $^{186}Os/^{188}Os$ ratios by Brandon et al. (1998, 1999) due to the presence of residual sulfides. However, PGE abundances in komatiites provide better tests of mantle source variations (e.g., Puchtel and Humayun, 2000, 2005).

A series of investigations have shown that the 2.8 Ga Kostomuksha komatiites have radiogenic initial $^{186}Os/^{188}Os$ and $^{187}Os/^{188}Os$ ratios relative to the 2.7 Ga Abitibi komatiites (Puchtel et al., 2004b; Puchtel et al., 2005). However, Kostomuksha komatiites show no excess PGE abundances (Puchtel and Humayun, 2005) relative to the Abitibi komatiites (Puchtel et al., 2004a). Does this refute core–mantle interaction? Puchtel and Humayun (2000) first concluded that these findings only refute a specific mechanism for core–mantle interaction: simple physical mixing of core and mantle. However, isotopic exchange of Os at the core–mantle boundary is not precluded by these data and provides a viable mechanism for core–mantle interaction (Puchtel and Humayun, 2005). Humayun et al. (2004) argued that decoupling of Fe/Mn from Os and W isotopic tracers of core–mantle interaction was consistent with a process of elemental and isotopic exchange at the core–mantle boundary. Thus, the arguments of Sobolev et al. (2005) do not constitute evidence against core–mantle interaction, only refutation of the specific mechanism of physical admixture (Walker et al., 1997; Brandon et al., 1998, 1999), a conclusion which has been accepted by Brandon and Walker (2005).

5. CONCLUSIONS

New data reported here refine and expand upon previous results in Humayun et al. (2004). Analyses of 14 MORB basalts from the Indian, Atlantic, and Pacific oceans by laser ablation ICP-MS reveals that the Fe/Mn ratio in MORB is 53–56, lower than the value obtained in Humayun et al. (2004) for solution nebulization ICP-MS analysis of the same samples. The highest Fe/Mn ratios are in Pacific MORBs. These new data agree well with the larger dataset of Langmuir and coworkers obtained by the Direct Current Plasma (DCP) technique and form coherent fractionation trends in a Fe/Mn vs. MgO plot. After correction for fractionation, MORB at MgO = 8% has Fe/Mn = 54. A high-MgO (15.17%) sample has Fe/Mn = 54.67, indicating that the mean Fe/Mn in MORB with 10–15% MgO is 54.0 ± 0.6 (1σ).

Analyses of Fe/Mn in 19 Icelandic picrites and basalts representing 13 volcanic centers yield a mean Fe/Mn = 60 ± 2, with one exception which has an Fe/Mn = 65.6. The majority of Icelandic samples exhibit

$FeO_T \sim 9$–10 wt%, except for lavas from Skirdufell (ERZ) which have $FeO_T = 11.2$ wt% similar to that of Kilauea, Hawaii. Since the MgO range of the Icelandic lavas is identical to that of the Hawaiian lavas, fractionation or partial melting alone clearly cannot explain the higher Fe/Mn observed in Hawaii.

Analyses of Fe/Mn ratios in OIB lavas from Reunion (1), St. Helena (3) and Tahiti (7), expand the number of high Fe/Mn plumes to three: Hawaii, Tahiti and possibly Reunion. All three plumes are associated with the Pacific and African superswells. St. Helena lavas exhibit lower Fe/Mn, comparable to Icelandic lavas, although this conclusion is based on only two samples with MgO < 5%.

Komatiites from Belingwe ($Fe/Mn = 58.3 \pm 0.2$, 1σ) and Gorgona ($Fe/Mn = 59$), however, do not show high Fe/Mn ratios (relative to Iceland). The Gorgona result is based on a single analysis and should be regarded as preliminary, until further analyses of Fe/Mn ratios of Gorgona komatiites are available. The Fe/Mn ratios (44–76) in Alexo komatiites were affected by alteration.

No clear relationship was found between high FeO_T (an indicator of depth of melting) and high Fe/Mn, even though the highest Fe/Mn ratios occur in high FeO_T lavas. For example, of six Icelandic lavas that show FeO_T 10.8–11.5%, only one has Fe/Mn > 65. Likewise, St. Helena lavas have 11.8% FeO_T (at 15% MgO) slightly higher than the Hawaiian lavas studied by Humayun et al. (2004), but Fe/Mn 62 ± 3 lower than Hawaiian lavas which have $Fe/Mn \sim 67$ (at 15% MgO).

Humayun et al. (2004) showed that experimental melts of fertile garnet lherzolite in the pressure range 3–7 GPa exhibit Fe/Mn ratios that are lower than their source, so that the high Fe/Mn ratios in Hawaii, Tahiti and Reunion are indicative of source compositions higher than 67 compared with normal mantle at about 60. A potential source of the high FeO in some plume-derived lavas is the outer core which is possibly saturated with FeO. Alternatively, the high Fe/Mn ratios of these plume-derived melts represent compositionally modified source regions devoid of olivine (Sobolev et al., 2005). Regardless of the origin of high Fe/Mn it forms a powerful new tool to explore source heterogeneity of major-elements in the mantle.

ACKNOWLEDGMENTS

Most of the samples for this research were made available by the National Museum of Natural History and we thank Sorena S. Sorenson and Leslie Hale for their help with these collections. Specific information on the NMNH MORB samples was provided by Tim O'Hearn. We are grateful to Alan D. Brandon for generously providing picrite sample powders from his Iceland collection, background information, encouragement and innumerable discussions. Komatiite sample powders were generously provided by Igor Puchtel (Alexo), Rich Walker (Gorgona, Belingwe) and Euan Nisbet (Belingwe). This research was partially supported by NSF grants EAR-0309786 and EAR-0509176 (MH) from Petrology & Geochemistry for which we are thankful. We appreciate helpful discussions with Francis Albarède, Shichun Huang, and Fred Frey, and an internal review from Shichun Huang. We thank Cin-Ty Lee, Alex Sobolev, Fred Frey, and an anonymous reviewer for their reviews, and Fred Frey for his diligent editorial handling.

APPENDIX 1A. SAMPLE INFORMATION PROVIDED BY THE SMITHSONIAN INSTITUTION FOR MORB BASALTIC GLASSES

Sample	Type	Location	Latitude, Longitude	Depth beneath sea water (m)
Pacific				
111240.0023	OCNGR68-D10	Blanco trough, Juan de Fuca ridge	44°40′00″N, 130°20′00″W	2220–2195
111240.0223	OCNGR68-D10	Blanco trough, Juan de Fuca ridge	44°40′00″N, 130°20′00″W	2220–2195
111240.0195	OCNGR68-D10	Blanco trough, Juan de Fuca ridge	44°40′00″N, 130°20′00″W	2220–2195
115199	KK78 12-D20	Galapagos Spreading Center	01°38′N, 094°57′W	3000
115739	KK78 12-D20	Galapagos Spreading Center	01°38′10″N, 094°57′10″W	2880
115200	KK78 12-D21	Galapagos Spreading Center	01°38′N, 094°58′58″W	3000
Dive 1376	Alvin Dive	East Pacific Rise	12.83°N, 103.95°W	2606
Indian				
115290	RSR79 D 2	Carlsberg Ridge	09°49′42″N,057°56′30″E; 09°49′12″N, 057°56′54″E	3347–3146
115294.0012	RSR79 D 7	Carlsberg Ridge	03°41′59″N, 063°53′31″E	3840–3749
115293.0002	RSR79 D 6	Carlsberg Ridge	03°47′00″N, 063°52′00″E	4023
VG6778	ANTP128		13°1′S, 066°19′E	1760–1885
Atlantic				
115089.0084	TW65-D10	Mid-Atlantic Ridge	22°17′N, 045°25′W; 22°19′N, 045°03′W	2590-3100
113021.0071	AII 60-2 1971	Mid-Atlantic Ridge	22°55′S, 013°30′W; 22°56′S, 013°32′W	3109–2195
115261	M7841	Mid-Atlantic Ridge	18°55′N, 046°01′W	2703–3100

APPENDIX 1B. SAMPLE INFORMATION FOR ICELANDIC PICRITES (FOR ADDITIONAL DETAILS, SEE BRANDON ET AL., 2007)

Sample	Group	Type	Location
ICE0	NRZ	Picrite	Hruthalsar
ICE2	WRZ	Picrite	Lagafell, shield volcano of Reykjanes (Holocene)
ICE3	WRZ	picrite	Stapafell, Reykjanes
ICE4a	WRZ	Picrite	Maelifell, Reykjanes
ICE4b	WRZ	Picrite	Maelifell, Reykjanes
ICE5	WRZ	Picrite	Dagmalafell, Reykjanes
DMF9101	WRZ	Picrite	Same as ICE5
ICE6	NRZ	Picrite	Theistareykir, shield volcano (Holocene)
ICE8a	ERZ	Picrite	Skridufell
ICE8b	ERZ	Picrite	Skridufell
ICE9a	ERZ	Picrite	Skridufell, flow above ICE8
ICE10	WRZ	Picrite	Hrudurkarlarnir
ICE11	WRZ	Picrite	Grindarik, Reykjanes
9805	WRZ	Picrite	Haleyjabunga, shield volcano of Reykjanes
9806	WRZ	Picrite	Vatnsheidi
9809	WRZ	Picrite	Fagradalshraun, Reykjanes
9810	WRZ	Basalt	Eldborg
9812	WRZ	Basalt	Asar, Reykjanes
9815	WRZ	Basalt	Lyngfell

Abbreviations: NRZ, northern rift zone; WRZ, western rift zone; ERZ, eastern rift zone.

APPENDIX 1C. SAMPLE INFORMATION ON TAHITI SAMPLES PROVIDED BY THE SMITHSONIAN INSTITUTION

Sample	Type	Location
100845	Basalt with porphyritic olivine	Collected in stream 5 km up Tiperui valley
100899		
100799	Basalt with porphyritic olivine	Collected above forks at first ridge of Fautaua River
100783	Basalt with porphyritic olivine	Collected from first dike cutting tuff at point TA HaRA
100866	Basalt with variolitic, porphyritic olivine	From Punaruu River
100842	Basalt, vesicular	Collected in stream at 4th crossing, tip Erui valley
100807	Basalt with olivine inclusion	Collected from stream at second bridge above forks Fautaua River

Appendix 1C (*continued*)

REFERENCES

Albarede F. (1992) How deep do common basaltic magmas form and differentiate? *J. Geophys. Res. B* **97**, 10,997–11,009.

Albarede F., Luais B., Fitton G., Semet M., Kaminski E., Upton B. G. J., Bachelery P. and Cheminee J.-L. (1997) The geochemical regimes of Piton de la Fournaise volcano (Réunion) during the last 530,000 years. *J. Petrol.* **38**, 171–201.

Anderson D. L. (1989) Composition of the Earth. *Science* **243**, 367–370.

Bennett V. C., Norman M. D. and Garcia M. O. (2000) Rhenium and platinum group element abundances correlated with mantle source components in Hawaiian picrites: sulfide in the plume. *Earth Planet. Sci. lett.* **183**, 513–526.

Bezos A. and Humler E. (2005) The $Fe^{3+}/\Sigma Fe$ ratios of MORB glasses and their implications for mantle melting. *Geochim. Cosmochim. Acta* **69**, 711–725.

Bijwaard H. and Spakman W. (1999) Tomographic evidence for a narrow whole mantle plume below Iceland. *Earth Planet. Sci. Lett.* **166**, 121–126.

Brandon A. D. and Walker R. J. (2005) The debate over core–mantle interaction. *Earth Planet. Sci. Lett.* **232**, 211–225.

Brandon A. D., Walker R. J., Morgan J. W., Norman M. D. and Prichard H. M. (1998) Coupled ^{186}Os and ^{187}Os evidence for core–mantle interaction. *Science* **280**, 1570–1573.

Brandon A. D., Norman M. D., Walker R. J. and Morgan J. W. (1999) ^{186}Os –^{187}Os systematics of Hawaiian picrites. *Earth Planet. Sci. Lett.* **174**, 25–42.

Brandon A. D., Walker R. J., Puchtel I. S., Becker H., Humayun M. and Revillon S. (2003) ^{186}Os and ^{187}Os systematics of Gorgona Island komatiites: implications for early growth of the inner core. *Earth Planet. Sci. Lett.* **206**, 411–426.

Brandon A. D., Graham D. W., Waight T. and Gautason B. (2007) ^{186}Os and ^{187}Os enrichments and high-$^{3}He/^{4}He$ sources in the Earth's mantle: evidence from Icelandic picrites. *Geochim. Cosmochim. Acta* **71**, 4570–4591.

Bryan W. B. (1983) Systematics of modal phenocryst assemblages in submarine basalts: petrologic implications. *Contrib. Mineral. petrol.* **83**, 62–74.

Campbell A. J. and Humayun M. (1999) Trace element micro-analysis in iron meteorites by laser ablation ICPMS. *Anal. Chem.* **71**, 939–946.

Campbell A. J. and Humayun M. (2005) Compositions of Group IVB iron meteorites and their parent melt. *Geochim. Cosmochim. Acta* **69**, 4733–4744.

Campbell A. J., Humayun M. and Weisberg M. K. (2002) Siderophile element constraints on the formation of metal in the metal-rich chondrites Bencubbin, Weatherford, and Gujba. *Geochim. Cosmochim. Acta* **66**, 647–660.

Canil D., O'Neill H. St. C., Pearson D. G., Rudnick R. L., McDonough W. F. and Carswell D. A. (1994) Ferric iron in peridotites and mantle oxidation states. *Earth Planet. Sci. Lett.* **123**, 205–220.

Courtillot V., Davaille A., Besse J. and Stock J. (2003) Three distinct types of hotspots in the Earth's mantle. *Earth Planet. Sci. Lett.* **205**, 295–308.

Daly R. A. (1927) The geology of Saint Helena Island. *Proc. Am. Acad. Arts Sci.* **62-2**, 92.

Dyar M. D., McGuire A. V. and Harrell M. D. (1992) Crystal chemistry of iron in two style of metasomatism in the upper mantle. *Geochim. Cosmochim. Acta* **56**, 2579–2586.

Henderson P. (1982) *Inorganic Geochemistry*. Pergamon Press Ltd., Oxford, UK (353 p.).

Hirschmann M. M., Baker M. B. and Stolper E. M. (1998) The effect of alkalis on the silica content of mantle-derived melts. *Geochim. Cosmochim. Acta* **62**, 883–902.

Hofmann A. W. (1997) Mantle geochemistry: the message from oceanic volcanism. *Nature* **385**, 219–229.

Huang S., Humayun M. and Frey F. A. (2007) Iron/manganese ratio and manganese content in shield lavas from Ko'olau Volcano, Hawai'i. *Geochim. Cosmochim. Acta* **71**, 4557–4569.

Humayun M., Puchtel I. S., Brandon A. D. (2002) PGEs in Icelandic picrites. *Geochim. Cosmochim. Acta* **66** (15A), A347–A347 (abstract).

Humayun M., Qin L. and Norman M. D. (2004) Geochemical evidence for excess iron in the mantle beneath Hawaii. *Science* **306**, 91–94.

Humayun M., Qin L., Brandon A. D. (2005) Implications of mantle Fe/Mn for mantle plumes. *Geochim. Cosmochim. Acta* **69** (10S), A104 (abstract).

Grove T. L. and Bryan W. B. (1983) Fractionation of pyroxene-phyric MORB at low pressure: an experimental study. *Contrib. Mineral. Petrol.* **84**, 293–309.

Jellinek A. M., Manga M. (2004) Links between long-lived hot spots, mantle plumes, D″, and plate tectonics. *Rev. Geophys.* **42**, RG3002/2004, 2003RG000144.

Klein E. M. and Langmuir C. H. (1987) Global correlations of ocean ridge basalt chemistry with axial depth and crustal thickness. *J. Geophys. Res. B* **92**, 8089–8115.

Lahaye Y., Arndt N., Byerly G., Chauvel C., Fourcade S. and Gruau G. (1995) The influence of alteration on the trace elements and Nd isotopic compositions of komatiites. *Chem. Geol.* **126**, 43–64.

Lahaye Y. and Arndt N. (1996) Alteration of a komatiite flow from Alexo, Ontario, Canada. *J. Petrol.* **37**, 1261–1284.

Langmuir C. H. and Hanson G. N. (1980) An evaluation of major element heterogeneity in the mantle sources of basalts. *Philos. Trans. R. Soc. London A* **297**, 383–407.

Laul J. C., Wakita H. and Showalter D. L. (1972) Bulk, rare earth, and other trace elements in Apollo 14 and 15 and Luna 16 samples. *Proc. Lunar Sci. Conf.* **3**, 1181–1200.

Lee C.-T. A. (2004) Are Earth's core and mantle on speaking terms? *Science* **306**, 64–65.

Lee C.-T. A., Yin Q., Lenardic A., Agranier A., O'Neill C. J. and Thiagarajan N. (2007) Trace-element composition of Fe-rich residual liquids formed by fractional crystallization: implications for the Hadean magma ocean. *Geochim. Cosmochim. Acta* **71**, 3601–3615.

Mao W. L., Mao H.-K., Sturhahn W., Zhao J., Prakapenka V. B., Meng Y., Shu J., Fei Y. and Hemley R. J. (2006) Iron-rich post-perovskite and the origin of ultralow-velocity zones. *Science* **312**, 564–565.

McDonough W. F. and Sun S.-s. (1995) The composition of the Earth. *Chem. Geol.* **120**, 223–253.

Melson W. G., O'Hearn T., Jarosewich E. (2002) A data brief on the Smithsonian abyssal volcanic glass data file. *Geochem. Geophys. Geosyst.* **3**, doi:10.1029/2001/GC000249.

Montelli R., Nolet G., Dahlen F. A., Masters G., Engdahl E. R. and Hung S.-H. (2004) Finite-frequency tomography reveals a variety of plumes in the mantle. *Science* **303**, 338–343.

Nielsen S. G., Rehkämper M., Norman M. D., Halliday A. N. and Harrison D. (2006) Thallium isotopic evidence for ferromanganese sediments in the mantle source of Hawaiian basalts. *Nature* **439**, 314–317.

Nisbet E. G., Arndt N. T., Bickle M. J., Cameron W. E., Chauvel C., Cheadle M., Hegner E., Kyser T. K., Martin A., Renner R. and Roedder E. (1987) Uniquely fresh 2.7 Ga komatiites from the Belingwe greenstone belt, Zimbabwe. *Geology* **15**, 1147–1150.

Norman M. D. and Garcia M. O. (1999) Primitive magmas and source characteristics of the Hawaiian plume: petrology and geochemistry of shield picrites. *Earth Planet. Sci. Lett.* **168**, 27–44.

Niu F., Solomon S. C., Silver P. G., Suetsugu D. and Inoue H. (2002) Mantle transition-zone structure beneath the South Pacific Superswell and evidence for a mantle plume underlying the Society hotspot. *Earth Planet. Sci. Lett.* **198**, 371–380.

Pickering-Witter J. and Johnston A. D. (2000) The effects of variable bulk composition on the melting systematics of fertile peridotitic assemblages. *Contrib. Mineral. Petrol.* **140**, 190–211.

Perfit M. R., Fornari D. J., Ridley W. I., Kirk P. D., Casey J., Kastens K. A., Reynolds J. R., Edwards M., Desonie D., Shuster R. and Paradis S. (1996) Recent volcanism in the Siqueiros transform fault: picritic basalts and implications for MORB magma genesis. *Earth Planet. Sci. Lett.* **141**, 91–108.

Puchtel I. S. and Humayun M. (2000) Platinum group elements in Kostomuksha komatiites and basalts: implications for oceanic crust recycling and core–mantle interaction. *Geochim. Cosmochim. Acta* **64**, 4227–4242.

Puchtel I. S. and Humayun M. (2001) PGE fractionation in a komatiitic basalt lava lake. *Geochim. Cosmochim. Acta* **65**, 2979–2993.

Puchtel I. S. and Humayun M. (2005) Highly siderophile element geochemistry of ^{187}Os-enriched 2.8 Ga Kostomuksha komatiites, Baltic Shield. *Geochim. Cosmochim. Acta* **69**, 1607–1618.

Puchtel I. S., Humayun M., Campbell A. J., Sproule R. A. and Lesher C. M. (2004a) Platinum group element geochemistry of komatiites from Alexo and Pyke Hill Areas, Ontario, Canada. *Geochim. Cosmochim. Acta* **68**, 1361–1383.

Puchtel I. S., Brandon A. D. and Humayun M. (2004b) Precise Pt–Re–Os isotope systematics of the mantle from 2.7-Ga komatiites. *Earth Planet. Sci. Lett.* **224**, 157–174.

Puchtel I. S., Brandon A. D., Humayun M. and Walker R. J. (2005) Evidence for the early differentiation of the core from Pt–Re–Os isotope systematics of 2.8 Ga komatiites. *Earth Planet. Sci. Lett.* **237**, 118–134.

Puchtel I. S., Brandon A. D., Walker R. J., Nisbet E. G. (2007) Pt–Re–Os isotope and HSE systematics of Belingwe komatiites. *Geochim. Cosmochim. Acta* **71** (15S), A812 (abstract).

Putirka K. D. (2005) Mantle potential temperatures at Hawaii, Iceland, and the mid-ocean ridge system, as inferred from olivine phenocrysts: evidence for thermally driven plumes. *Geochem. Geophys. Geosyst.* **6**, doi:10.1029/2005GC000915.

Ravizza G., Blusztajn J. and Prichard H. M. (2001) Re–Os systematics and platinum – group element distribution in

metalliferous sediments from the Troodos ophiolite. *Earth Planet. Sci. Lett.* **188**, 369–381.

Reinitz I. and Turekian K. K. (1989) $^{230}Th/^{238}U$ and $^{226}Ra/^{230}Th$ fractionation in young basaltic glasses from the East Pacific Rise. *Earth Planet. Sci. Lett.* **94**, 199–207.

Revillon S., Arndt N. T., Chauvel C. and Hallot E. (2000) Geochemical study of ultramafic volcanic and plutonic rocks from Gorgona island, Colombia: the plumbing system of an oceanic plateau. *J. Petrol.* **41**, 1127–1153.

Rhodes J. M. and Vollinger M. J. (2005) Ferric/ferrous ratios in 1984 Mauna Loa lavas: a contribution to understanding the oxidation state of Hawaiian magmas. *Contrib. Mineral. Petrol.* **149**, 666–674.

Rubie D. C., Gessmann C. K. and Frost D. J. (2004) Partitioning of oxygen during core formation on the Earth and Mars. *Nature* **429**, 58–61.

Russell S. S., Lay T. and Garnero E. J. (1998) Seismic evidence for small-scale dynamics in the lowermost mantle at the root of the Hawaiian hotspot. *Nature* **396**, 255–258.

Ruzicka A., Snyder G. A. and Taylor L. A. (2001) Comparative geochemistry of basalts from the Moon, Earth, HED asteroid, and Mars: implications for the origin of the Moon. *Geochim. Cosmochim. Acta* **65**, 979–997.

Shen Y., Wolfe C. J. and Solomon S. C. (2003) Seismological evidence for a mid-mantle discontinuity beneath Hawaii and Iceland. *Earth Planet. Sci. Lett.* **214**, 143–151.

Sobolev A. V., Hofmann A. W., Sobolev S. V. and Nikogosian I. K. (2005) An olivine-free mantle source of Hawaiian shield basalts. *Nature* **434**, 590–597.

Sobolev A. V., Hofmann A. W., Kuzmin D. V., Yaxley G. M., Arndt N. T., Chung S.-L., Garcia M. O., Gurenko A. A., Danyushevsky A. C., Elliott T., Frey F. A., Kamenetsky V. S., Kerr A. C., Krivolutskaya N. A., Matvienkov V. V., Nikogosian I. K., Rocholl A., Suschevskaya N. M. and Teklay M. (2007) The amount of recycled crust in sources of mantle-derived melts. *Science* **316**, 412–417.

Stolper E., Sherman S., Garcia M., Baker M., Seaman C. (2004) Glass in the submarine section of the HSDP2 drill core, Hilo, Hawaii. *Geochem. Geophys. Geosys.* **5**, Q07G15, doi:10.1029/2003GC000553.

Takafuji N., Hirose, K., Mitome, M., Bando, Y. (2005) Solubilities of O and Si in liquid iron in equilibrium with (Mg, Fe)SiO_3 perovskite and the light elements in the core. *Geophys. Res. Lett.* **32**, L06313, doi:10.1029/2005GL022773.

Walker D. (2000) Core participation in mantle geochemistry. *Geochim. Cosmochim. Acta* **64**, 2897–2911.

Walker R. J., Morgan J. W., Beary E., Smoliar M. I., Czamanske G. K. and Horan M. F. (1997) Applications of the ^{190}Pt-^{186}Os isotope system to geochemistry and cosmochemistry. *Geochim. Cosmochim. Acta* **61**, 4799–4808.

Walker R. J. and Nisbet E. G. (2002) ^{187}Os isotopic constraints on Archean mantle dynamics. *Geochim. Cosmochim. Acta* **66**, 3317–3325.

Walter M. J. (1998) Melting of garnet peridotite and the origin of komatiite and depleted lithosphere. *J. Petrol.* **39**, 29–60.

Wolfe C. J., Bjarnason I. T., Van Decar J. C. and Solomon S. C. (1997) Seismic structure of the Iceland mantle plume. *Nature* **385**, 245–247.

Zindler A. and Hart S. R. (1986) Chemical geodynamics. *Ann. Rev. Earth Planet. Sci.* **14**, 493–571.

Associate editor: Frederick A. Frey